

## Partial screening in Ca silicides measured by Ca 2p electron-energy-loss spectroscopy

Massimo Sancrotti

*Laboratorio Tecnologie Avanzate Superfici e Catalisi, Istituto Nazionale per la Fisica della Materia, Padriciano 99, I-34012 Trieste, Italy*

Lucia Calliari\* and Fabio Marchetti

*Divisione Scienza dei Materiali, Istituto per la Ricerca Scientifica e Tecnologica, I-38050 Povo, Italy*

Francesco Rapisarda† and Olmes Bisi

*Dipartimento di Fisica, Università di Trento, I-38050 Povo, Italy*

A. Iandelli, G. L. Olcese, and A. Palenzona

*Istituto di Chimica-Fisica, Università di Genova, Corso Europa 32, I-16130 Genova, Italy*

(Received 20 June 1994)

We report Ca 2p electron-energy-loss spectra (EELS) of Ca silicides (Ca<sub>2</sub>Si, CaSi, CaSi<sub>2</sub>) for various primary electron-beam energies ( $E_p = 565, 800, 1046, \text{ and } 1500 \text{ eV}$ ). For fixed primary energy, the Ca 2p profiles are found to be very similar regardless of the site-specific environment. The high-energy excited EELS spectra bear a strong resemblance to the Ca 2p x-ray-absorption spectra (XAS) of Ca metal and CaSi<sub>2</sub>, while the low-primary-energy spectra are characterized by a strong transfer of spectral weight toward the threshold and an inversion of the  $2p_{1/2}$  vs  $2p_{3/2}$  branching ratio. Whatever the primary energy is, the EELS spectra are found to strongly deviate from Ca 2p spectra calculated in a pure bandlike approach (ground-state calculation). An insight into the role of screening effects is achieved via the calculation of the absorption profile of Ca metal excited by the presence of the 2p core hole. While the ground-state calculation accounts for the nonscreened system, the excited one describes a fully screened atom. We show that both the XAS and the high-energy EELS spectra reflect a configuration of partial screening of the 2p core hole. The strong transfer of spectral weight toward the threshold found in the low-primary-energy EELS spectra are interpreted in terms of a more complete screening due to the participation of the slower injected electron. Therefore, the degree of screening can be driven by varying the final-state energy of the injected electron.

### I. INTRODUCTION

X-ray absorption spectroscopy and core-level electron-energy-loss spectroscopy are well-known techniques allowing one to probe the unoccupied electronic structure of solids local to the core-hole excited atomic site.<sup>1</sup> Various regimes of behavior have been reported. In the case of highly localized final states [rare earth (RE) 4f or actinide 5f], the spectra are satisfactorily interpreted in terms of atomiclike multiplets<sup>2,3</sup> whereas x-ray absorption spectroscopy (XAS) of the heavier 3d transition metals (TM's) and of a wide series of other systems has been established to mimic the distribution of partial density of states (PDOS) somehow modulated by matrix element effects.<sup>4,5</sup> The variety of spectroscopic behavior is by far richer than suggested by the aforementioned examples. In many cases, atomiclike and bandlike aspects actually competitively coexist in the spectroscopic excitation response. This is, for instance, the case of the lighter 3d TM's.<sup>4,6,7</sup> A crucial point in such situations deals with how to discriminate between solid- and atomic-state properties. In this context, XAS electron-energy loss spectroscopy (EELS) of Ca and Ca-containing systems is extremely relevant. It has been theoretically and experimentally established that in ionic Ca-based compounds

different atomic environments local to the Ca sites determine, via crystal-field effects, great changes in the Ca 2p near-edge profile.<sup>7,8</sup> On this basis, surface- and interface-specific Ca-site geometries have been identified by exploiting the so-called search-of-light effect.<sup>8</sup> In addition, high-resolution Ca 2p XAS has been recently proven to be powerful in obtaining insight over the unoccupied electronic structure of high-temperature superconductors.<sup>9</sup> It is thus interesting to investigate whether and how the Ca 2p XAS line shape changes in metalliclike compounds within a stoichiometric series as the chemical bond experienced by the Ca atoms is gradually changing.

In this paper, we report on a systematic investigation of the Ca 2p near-edge EELS profiles within the whole stoichiometric Ca silicide family (Ca<sub>2</sub>Si, CaSi, and CaSi<sub>2</sub>). EELS spectra have been measured at different selected values of the primary electron beam ranging from 1.5 to 4 times the binding energy value of the Ca 2p level. At each primary energy the Ca 2p EELS profiles appear very similar to each other regardless of the sizable changes occurring in the chemical environment local to the Ca sites. Moreover, a strong evolution of the very-near-edge line shape is found in Ca-containing systems as the primary energy is varied for each of the Ca silicides. This effect is discussed in terms of the transition from the sud-

den to the adiabatic limit of core-level excitation as the primary electron-beam energy is lowered towards the Ca  $2p$  BE threshold.

The comparison of the high-energy excited EELS spectra of Ca silicides with Ca  $2p$  XAS profiles of Ca metal and  $\text{CaSi}_2$  (Ref. 8) shows the similarity of the XAS and EELS spectra. Furthermore, it will allow us to discuss the relative role of electron- versus photon-induced excitation in determining the spectroscopic response.<sup>10–12</sup>

Both the EELS and XAS spectra cannot be interpreted within a bandlike scheme. This result agrees with the findings of Zaanen *et al.*<sup>6</sup> which suggest a strong screening effect in Ca metal. To investigate the possible role of screening effects in Ca metal we computed parameter-free theoretical XAS of Ca in the presence of a  $2p$  hole. Our calculation shows the effect of the attractive potential of the core hole with a shift of the absorption structures toward the threshold. The comparison with the experiment will show that both the XAS and high-energy EELS spectra reflect a configuration of partial screening of the  $2p$  core hole. The low-primary-energy EELS spectra are interpreted in terms of a more complete screening due to the participation of the slower injected electron.

Ca silicides are relevant for a wide variety of reasons. Firstly, a thorough experimental [photoemission (PES), bremsstrahlung isochromat (BIS), and Auger spectroscopies] and theoretical investigation of their occupied as well as empty electronic structure has been reported.<sup>13–16</sup> Moreover, the distribution of electron states changes markedly while moving within the family of Ca silicides. Therefore, they appear as a good test bench for newly developed or more exotic spectroscopies as is the case of core-level EELS. Secondly, a Ca silicidelike environment is known to occur at the  $\text{Si}(111)/\text{CaF}_2$  epitaxial interface which is extremely relevant to three-dimensional packaging<sup>17,18</sup> and moreover  $\text{CaSi}_2$  epilayers have been grown on  $\text{Si}(111)$  substrates.<sup>19</sup> Thirdly, Ca silicides have been demonstrated to be reliable prototypical systems for in-depth understanding of the chemical-bond evolution within the RE silicides series.<sup>20–22</sup>

## II. EXPERIMENT

The Ca silicides have been prepared by melting stoichiometric amounts of the atomic components in refractory crucibles with inert gas atmosphere. Phase homogeneity and structures have been checked via metallographic and x-ray diffraction analysis. Extra phases were below the limit of 3%.

Clean surfaces have been obtained by scraping with a diamond file in ultrahigh vacuum. The pressure ranged from  $1 \times 10^{-10}$  (base value) to  $7 \times 10^{-10}$  mbar during filing. EELS spectra were excited with an electron gun and measured in a reflection and angle-integrating mode by a coaxial double-pass cylindrical mirror analyzer (CMA) operated in the nonretarding mode for all the primary beam energies ( $E_p = 565, 800, \text{ and } 1046 \text{ eV}$ ) except from the highest value ( $E_p = 1500 \text{ eV}$ ). The typical energy resolution of the CMA amounted to about 0.6 ( $E_p = 565$ ), 1.35 ( $E_p = 800$ ), 2.1 ( $E_p = 1046$ ), and 1.2 eV

( $E_p = 1500 \text{ eV}$ ). Current densities were of the order of  $10^3 - 10^4 \text{ A/m}^2$ , depending on the primary-energy value. Due to the reactivity of the Ca silicide surfaces with the residual gas under prolonged electron bombardment, periodic checks of the surface cleanliness were performed via Auger spectroscopy. For the herein reported EELS spectra, typical contaminants were below 3%. This ensures us that none of the line-shape evolutions are due to artifacts. The longest data acquisition time was about 120 min. Long acquisition times are needed to achieve good statistics spectra because of the low-amplitude values of the signal compared with the underlying secondary-electron background. Spectra, not shown here, were also acquired with the primary-beam energies some eV lower than the aforementioned values so as to ensure us of the absence of any Auger-related Si- or Ca-specific structure in the kinetic energy ranges where the Ca  $2p$  EELS structures were expected.

## III. THEORY

The electronic properties of calcium metal and Ca silicides were calculated from first principles by the linear muffin-tin orbitals method in the atomic-spheres approximation.<sup>23</sup> The local-density approximation to the density-functional formalism<sup>24</sup> is the underlying framework. The core-electron energies and wave functions were evaluated from the potential energy in the solid, at every step of the self-consistent iterative procedure, i.e., without the so-called frozen-core approximation.

We performed two types of calculations. The first one is a standard band-structure calculation, i.e., a ground-state one, giving a band structure in agreement with the published results.<sup>25</sup> The second one, performed on Ca metal, is a band-structure calculation with the explicit inclusion of the core hole involved in the x-ray transition. In this set of calculations the excited atom is formally treated as an impurity, in order to self-consistently describe the charge redistribution induced by the core-hole potential. This impurity problem has been self-consistently solved with a supercell technique.<sup>26</sup> Our supercell contained 27 Ca atoms, i.e., it was 27 times bigger than the unit cell, which corresponds to the choice of a lattice constant three times bigger than the usual one.<sup>27</sup> The supercell should be large enough to prevent any interaction between excited atoms in neighboring supercells.<sup>26</sup> A smaller supercell (for instance, a supercell made of eight unit cells) suffers from such size effects. The neutrality of the supercell was ensured by adding the extracted core electron to the valence states. In the calculations the expansion of the single-particle wave functions was carried up to  $l=2$ . The state densities were determined by the tetrahedron technique<sup>28</sup> starting from energy levels computed over a uniform mesh. 946 points in the irreducible wedge of the first Brillouin zone were used in the case of the ground-state calculations while 50 points were used in the case of the supercell calculations (in this case, the number of  $k$  points decreases in order to have approximately the same sampling of the reciprocal space as in the ground-state calculations).

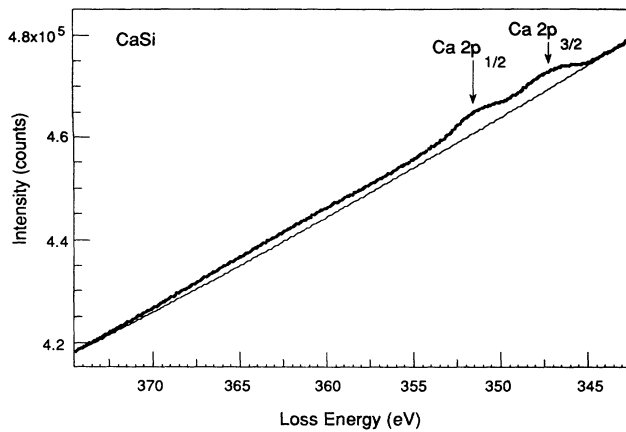


FIG. 1. As-measured Ca  $2p$  EELS spectrum ( $E_p = 800$  eV) of CaSi. Also shown is the background line as discussed in the text.

#### IV. RESULTS AND DISCUSSION

Figure 1 gives an example of an as-acquired EELS spectrum excited at the Ca  $2p$  threshold ( $E_p = 800$  eV) from one of the investigated Ca silicides, namely, CaSi (dots). Also shown is the typical background line (solid line), to be subtracted from the raw data and representing the contribution of secondary scattered electrons. Thus Fig. 1 gives an idea of the most critical aspect of the herein reported measurements, i.e., the high value of the background compared with the typical amplitude of the relevant near-edge signal. The vertical bars indicate the peak position of the structures which are due to the Ca  $2p_{1/2}$  and Ca  $2p_{3/2}$  spin-orbit-split contributions. More

details on the spectroscopic assignments of the EELS features will be given further below. The background line was obtained by fitting, via a second-order polynomial, the points located in the 5-eV-wide prethreshold region and the 1-eV-wide interval at about 30 eV above the near-edge structures. Different choices of the degree and energy limits defining the polynomial line were tested. The thus-obtained background-subtracted profiles were obviously dependent on the choices of the parameters. However, the trends observed here by changing the Ca silicide stoichiometry and primary electron-beam energy were not affected by these choices. Therefore we confine ourselves to show spectra obtained by subtracting a background such as that displayed in Fig. 1.

Figures 2–5 give near-edge background-subtracted EELS spectra excited at the Ca  $2p$  threshold for the various Ca silicides. Each figure corresponds to a differently selected value of the primary excitation energy. In the case of the two higher primary energies, the intermediate stoichiometry (CaSi) was not measured. Two observations are immediately evident. Firstly, for a specific choice of the primary energy the EELS profiles are very close in shape to each other regardless of the particular Ca silicide stoichiometry. Secondly, we notice an evolution of the EELS line shape as the primary energy is varied. In particular, the intensity of the Ca  $2p_{3/2}$  structure decreases relative to the Ca  $2p_{1/2}$  component as the primary energy is increased. This occurs when going from  $E_p = 565$  up to 1046 eV (Figs. 2–4) whereas no significant further change is noticed when comparing the two high-energy sets of EELS line shapes of Figs. 4 and 5. We also note that the energy separation of the two main peaks amounts to the same value for  $E_p = 1046$  and 1500

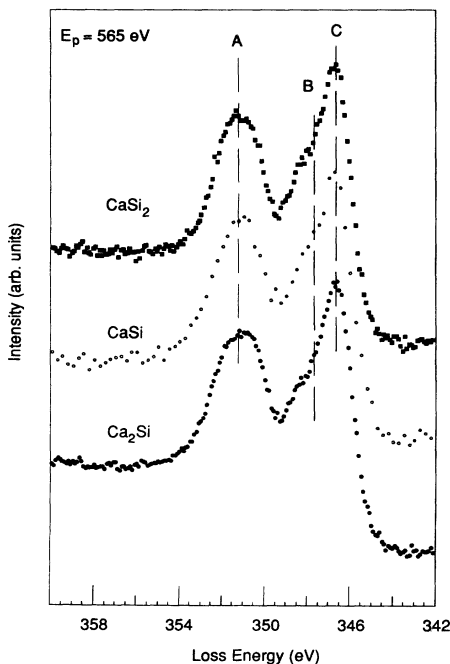


FIG. 2. Background-subtracted Ca  $2p$  EELS spectra of Ca silicides with  $E_p = 565$  eV.

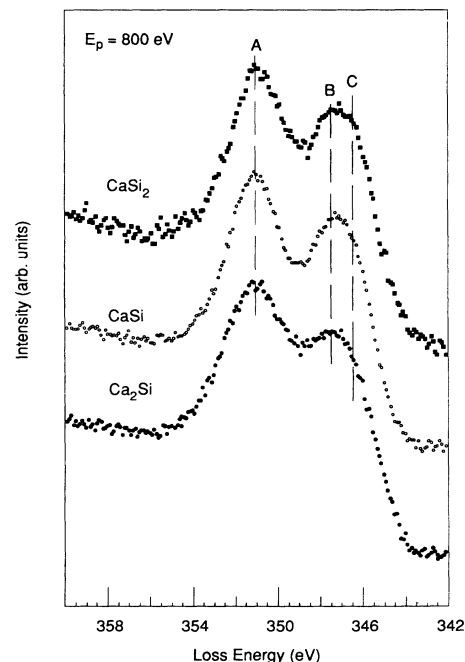


FIG. 3. Background-subtracted Ca  $2p$  EELS spectra of Ca silicides with  $E_p = 800$  eV.

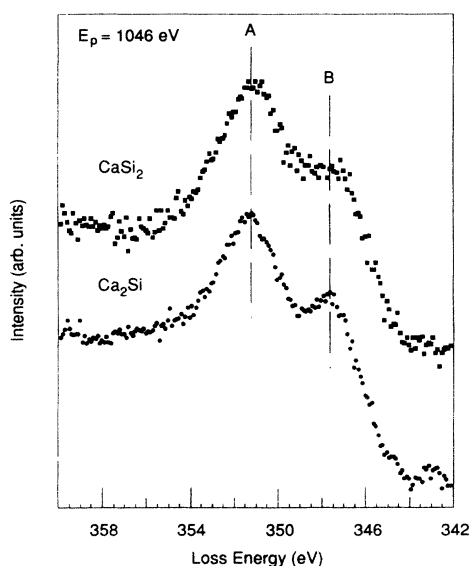


FIG. 4. Background-subtracted Ca 2p EELS spectra of Ca silicides with  $E_p = 1046$  eV.

eV. Moreover, in the case of the lowest primary energy (565 eV) three features are clearly resolved, as indicated in Fig. 2 by the vertical bars. Two structures marked *A* and *B* can be recognized in all the spectra and their energy location can be considered, not depending on  $E_p$ . The extra peak (*C*) emerges very close to the Fermi level when  $E_p$  is set at the lower limit herein reported. For  $E_p = 800$  eV it is not possible to separately resolve the features *B* and *C* and their energy position must be considered approximated.

Within the Born approximation, the EELS differential cross section  $d^2\sigma_{\text{EELS}}(E, q)/dE dq$ , in conditions of high incident energy and very low electron momentum ( $\Delta q$ )

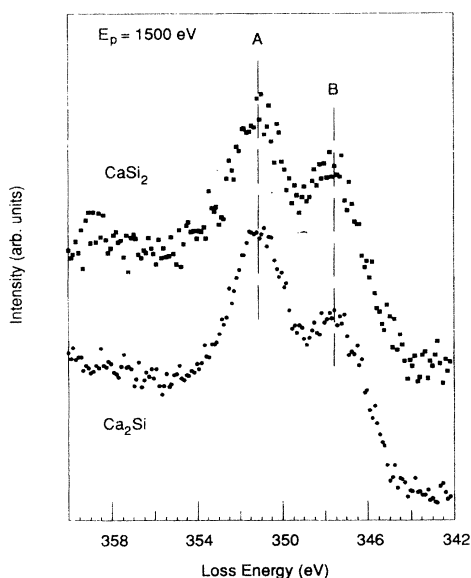


FIG. 5. Background-subtracted Ca 2p EELS spectra of  $\text{Ca}_2\text{Si}$  and  $\text{CaSi}_2$  with  $E_p = 1500$  eV.

transfer ( $\Delta q \ll 1/r_c$  where  $r_c$  is the mean radius of the core-level orbital), is equal to the XAS differential cross section  $d^2\sigma_{\text{XAS}}(E, q)/dE dq$ .<sup>29,30</sup> Solid confirmations to this are provided by the data for a wide variety of atomic species in different chemical bond configurations.<sup>31</sup> Moreover, similarity between core-level  $d^2\sigma_{\text{EELS}}(E, q)/dE dq$  and  $d^2\sigma_{\text{XAS}}(E, q)/dE dq$ , both in the near-edge and extended fine-structure regions, was also obtained for wider experimental conditions.<sup>31</sup> We note that some exceptions<sup>11,12,32,33</sup> were found. In particular, the EELS versus XAS similarity was found when EELS spectra are collected in the reflection mode with angle-integrating energy analyzers (e.g., CMA), as in our case. Efforts are being currently developed in order to define the validity and limits of the equivalency between XAS and EELS for a wide number of core levels and atomic species.<sup>10</sup> The case of *L*-shell excitation of low-*Z* elements has been proven to fall in the dipole regime for reflection-geometry EELS.<sup>10</sup> On this basis and taking into account the primary energy-independent line shapes of Figs. 4 and 5, we interpret the EELS profiles obtained with high-energy primary excitation ( $E_p = 1046$  and 1500 eV) as governed by the same physical mechanism typical of XAS. The adequateness of this approach is confirmed *a posteriori* by the similarity in the shape of our measured EELS profiles and the XAS spectra of Ca metal and  $\text{CaSi}_2$  measured by Himpsel *et al.*<sup>8</sup> We note that in this case  $E_p$  is more than four times the pertinent Ca 2p threshold energy.

On a pure bandlike approach, the Ca 2p EELS profiles of Ca metal and Ca silicides are expected to primarily reflect the unoccupied Ca 4(*sp*) and 3*d* density of states (DOS) projected onto the Ca sites as dictated by the  $l \rightarrow (l \pm 1)$  dipole selection rules. Since the  $l \rightarrow (l + 1)$  is by far the strongest contribution, the 3*d* DOS of the unoccupied state is the dominant one. Such PDOS's have been self-consistently calculated within the Andersen linear muffin-tin orbitals method in the atomic-sphere approximation and reported in Refs. 14 and 15. The validity of such single-particle calculations in the case of Ca silicides, as far as the different angular symmetries and atomic sites are concerned, has been extensively proved by photon energy-dependent BIS measurements for the empty portion of electronic states<sup>14,15</sup> and by synchrotron radiation PES and Si  $L_{2,3}VV$  Auger line-shape analysis on the occupied state side.<sup>13,16</sup> For the sake of comparison, theoretical Ca 2p EELS profiles have been synthesized from the computed Ca 3*d*-derived PDOS's of the whole Ca silicide series and shown in Fig. 6 (curves a). These curves have been obtained by taking into account the appropriate Ca 2p spin-orbit splitting ( $\Delta_{\text{SO}} = 3.7$  eV) and assuming a statistical value ( $= \frac{1}{2}$ ) in the Ca 2p<sub>1/2</sub> and 2p<sub>3/2</sub> relative intensity ratio. In the case of  $\text{Ca}_2\text{Si}$ , which is characterized by two families of nonequivalent Ca sites, we show the average.<sup>35</sup> Also shown in Fig. 6 are the Lorentzian ( $\gamma = [0.1 + 0.1(E - E_F)]$  (eV)) and Gaussian ( $\sigma = 0.865$  eV) broadened versions of the Ca 2p EELS profiles, simulating both lifetime<sup>4,6,36</sup> and instrumental effects (curves b). From the comparison between the measured spectra

(Figs. 4 and 5) and the computed one (Fig. 6), it is evident that a pure bandlike picture is definitely invalidated. In particular, stoichiometry-specific changes are predicted in the single-particle scheme whereas the experimentally determined spectra are very similar in shape. Moreover, the calculated line shapes strongly deviate from the measured profiles for each stoichiometry. The inclusion of the matrix elements effects, not considered in the data shown in Fig. 6, is not expected to modify this conclusion.<sup>34</sup> All these facts reveal the inadequacy of a pure bandlike approach for interpreting the Ca  $2p$  EELS and XAS spectra and suggest the occurrence of many-body effects. Our result on the importance of many-body effects in the EELS and XAS spectra of Ca silicides is similar to that found by Zaanen *et al.*<sup>6</sup> for Ca metal. This similarity is expected since the Ca EELS and XAS spectra do not show appreciable changes on varying the Ca stoichiometry and in going from  $\text{CaSi}_2$  to Ca metal.<sup>8</sup> In Ca metal, Zaanen *et al.*<sup>6</sup> suggest a strong screening effect due to the  $2p$  hole. They are able to interpret the experimental XAS spectrum by assuming an abnormally large value (3 eV) of the monopole ( $F_0$ )  $p$ - $d$  Coulomb interaction. The influence of the attractive  $F_0$  interaction is to increase the spectral weight on the low-energy side of the  $d$ -band density of states. Since this agreement is parameter dependent, it is important to investigate the screening effect in a parameter-free approach. We performed this analysis with the supercell calculation described previously. To have a better comparison with the

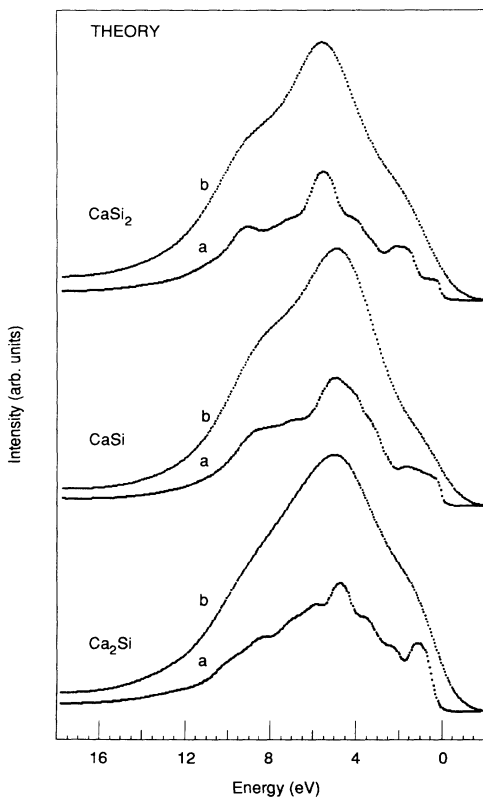


FIG. 6. Ca  $2p$  absorption spectra of Ca silicides as calculated under a pure bandlike approach. Curves a, nonbroadened profiles; curves b, broadened profiles.

experiment, we computed the complete XAS spectrum, including matrix-element effects.

Figure 7 gives two theoretical  $2p$  absorption profiles of Ca metal as calculated (i) by assuming the ground-state electronic structure (curve a) and (ii) by taking into account the effect of the core hole and of the screening charge (curve b). These calculated profiles, which include matrix-element effects, are shown after Lorentzian and Gaussian broadening. For comparison, also shown is the Ca  $2p$  XAS line shape of Ref. 8 and the highest- ( $E_p = 1500$  eV) and lowest-energy ( $E_p = 565$  eV) EELS spectra of  $\text{Ca}_2\text{Si}$ , i.e., the Ca-rich silicide. It can be immediately recognized that the center of gravity of the structures of the XAS and high-energy EELS spectra lie at energy positions which are intermediate between those predicted by the two calculations. Moreover, both the calculations fail in predicting the relative intensity of the  $2p_{1/2}$  versus  $2p_{3/2}$  components. In contrast, the low-energy EELS profile appears in much better agreement with the fully screened calculation both for the energy location of the structures and the distribution of spectral weight over the two spin-orbit split components. Moreover, an overall similarity in the shape of the fine structure at the  $2p_{3/2}$  component is recognized in both the fully screened calculation and the low-energy EELS spectra. The comparison with the  $2p_{1/2}$  component is somehow

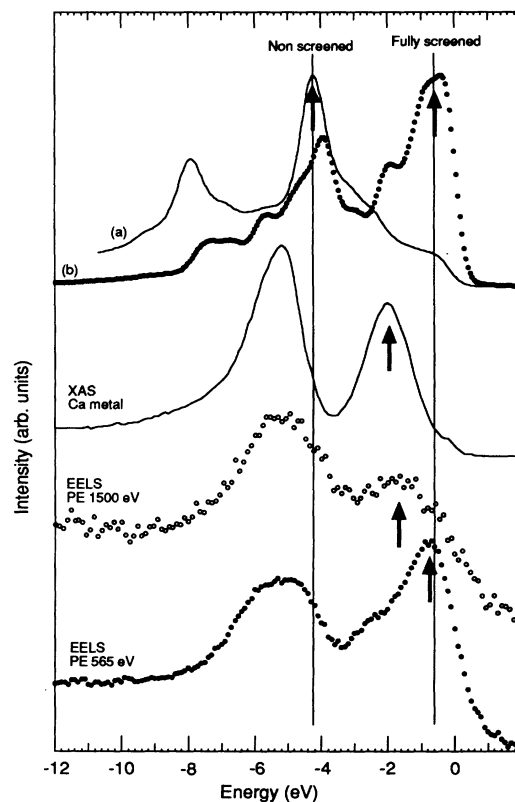


FIG. 7. Ca  $2p$  absorption profiles of Ca metal as calculated neglecting (curve a) and including (curve b) the core hole. Also shown are the XAS spectrum of Ca metal as measured by Himpsel *et al.* (Ref. 8) and two EELS spectra of  $\text{Ca}_2\text{Si}$  corresponding to high- and low-primary-beam energies. See the text for more details on the calculations.

hindered by the higher lifetime broadening effect acting at that threshold due to the occurrence of a deexcitation Coster-Kronig transition. Our interpretation of these results is the following: the condition of full screening around the Ca  $2p$  holes can be reached in EELS spectra. It crucially depends on the final-state energy of the extra electron typical of the EELS experiment and completely absent in XAS.

The role of the injected electron in determining the near-threshold C  $1s$  EELS line shape has been recently recognized<sup>32</sup> in diamond in a regime of pure dipole excitation. It has been actually demonstrated that the presence of the extra electron and related charge-density wake can drastically modify the core-exciton envelope function.

A primary-energy-dependent line-shape evolution of  $2p$  EELS spectra similar to that of Ca silicides has been reported by Powell and Erickson<sup>37,38</sup> for Ti, V, and Cr metals, i.e., the  $3d$  transition metals immediately following Ca in the  $3d$  row. In these cases, a narrow huge extra peak has been observed to grow up very close on the low-energy side of the  $2p_{3/2}$ -related structure as the primary energy was lowered down to about 50 eV above the  $2p$  threshold. This behavior has been postulated as reflecting a slow transition from sudden to adiabatic excitation conditions. We find consistency between this interpretation and the comments drawn from our analysis of Fig. 7: the low-primary-energy EELS spectra reflect a relaxed electronic configuration (adiabatic limit).

In principle, a series of arguments other than the extra-electron-induced screening effect could be invoked trying to explain the primary energy-dependent evolution of the EELS line shape.

(i) Surface effects—Low-primary-energy EELS spectra correspond to a higher surface sensitivity. Thus, progressively increasing contributions due to surface atoms are expected to be measured along with the bulk-related signal as the primary energy is lowered. Since surface atoms are different with respect to the bulk ones, an energy-dependent evolution of the EELS spectra is expected. However, such an effect cannot account for the measured inversion of  $2p_{1/2}$  versus  $2p_{3/2}$  spectral weight distribution.

(ii) Nondipole effects—It is well known<sup>10,11,31</sup> that as the primary energy approaches the core-level threshold energy the dipole limit is progressively invalidated and nondipole contributions are expected in the spectra. However, such contributions are not compatible with the measured line-shape evolution (the emergence of the structure  $A$  of Figs. 2 and 3). Nondipole contributions would actually cause electron states of angular momentum symmetry other than the  $3d$  one to be switched on in the EELS spectra. On the other hand, neither of these extra contributions are expected to give significant contribution to the near-edge structures since the empty states of Ca we investigated are primarily of  $3d$  symmetry. On this basis, the dynamical screening charge appears to play the dominant role in the specific primary energy-dependent Ca  $2p$  line-shape evolution.

## V. CONCLUSIONS

We have reported a systematic Ca  $2p$  EELS measurement of Ca silicides and a theoretical analysis of the non-screened and fully screened Ca system. For fixed primary electron-beam energy, the EELS profiles are very similar regardless of the specific stoichiometry showing the importance of the core-hole attractive potential. All the measured Ca  $2p$  EELS line shapes are found to markedly depend on the primary electron-beam energy. High-primary-energy EELS spectra are similar to the Ca  $2p$  XAS spectra. The comparison with the calculation shows that both spectroscopies probe a partially screened system. In contrast, low-primary-energy EELS spectra are in good agreement with the fully screened calculated absorption spectra. The relevant issue of defining the validity and limits of the equivalence between XAS and EELS has been therefore positively resolved in Ca-based systems.

## ACKNOWLEDGMENTS

Calculations have been performed at CISCA, University of Trento. This work was partially supported by the Consiglio Nazionale delle Ricerche under Grant No. 93.01619.PF69.

\*Present address: Centro Materiali e Biofisica Medica, Povo, Italy.

†Present address: Dipartimento di Fisica Teorica, Università di Trieste, Trieste, Italy.

<sup>1</sup>See, for example, *X-Ray Absorption: Principles, Applications, Techniques of EXAFS, SEXAFS and XANES*, edited by R. Prins and D. Koningsberger (Wiley, New York, 1988); *Photoemission and Absorption Spectroscopy of Solids and Interfaces*, edited by M. Campagna and R. Rosei (North-Holland, Amsterdam, 1990); *Unoccupied Electronic States*, edited by J. C. Fuggle and J. E. Inglesfield (Springer-Verlag, Berlin, 1992).

<sup>2</sup>F. P. Netzer, G. Strasser, and J. A. D. Matthew, *Phys. Rev. Lett.* **51**, 211 (1983); J. A. D. Matthew, G. Strasser, and F. P. Netzer, *Phys. Rev. B* **27**, 5839 (1983).

<sup>3</sup>B. T. Thole, G. van der Laan, J. C. Fuggle, G. A. Sawatzky, R. C. Karnatak, and M.-M. Esteva, *Phys. Rev. B* **32**, 5107 (1985).

<sup>4</sup>J. Fink, Th. Müller-Heinzerling, B. Scheerer, W. Speier, F. U. Hillebrecht, J. C. Fuggle, J. Zaanen, and G. A. Sawatzky, *Phys. Rev. B* **32**, 4899 (1985).

<sup>5</sup>P. Aebi, J. Keller, M. Erbudak, and F. Vanini, *Phys. Rev. B* **38**, 5392 (1988).

<sup>6</sup>J. Zaanen, G. A. Sawatzky, J. Fink, W. Speier, and J. C. Fuggle, *Phys. Rev. B* **32**, 4905 (1985).

<sup>7</sup>F. M. F. de Groot, J. C. Fuggle, B. T. Thole, and G. A. Sawatzky, *Phys. Rev. B* **41**, 928 (1990).

<sup>8</sup>F. J. Himpsel, U. O. Karlsson, A. B. McLean, L. J. Terminello, F. M. F. de Groot, M. Abbate, J. C. Fuggle, J. A. Yarmoff, B.

- T. Thole, and G. A. Sawatzky, *Phys. Rev. B* **43**, 6899 (1991).
- <sup>9</sup>A. Borg, P. L. King, I. Lindau, D. B. Mitzi, A. Kapitulnik, A. V. Soldatov, S. Della Longa, and A. Bianconi, *Phys. Rev. B* **46**, 8487 (1992); M. Qvarford, J. N. Andersen, R. Nyholm, J. F. van Acker, E. Lundgren, I. Lindau, S. Söderholm, H. Bernhoff, U. O. Karlsson, and S. A. Flodström, *ibid.* **46**, 14 126 (1992).
- <sup>10</sup>D. K. Saldin, *Phys. Rev. Lett.* **60**, 1197 (1988); D. K. Saldin and Y. Ueda, *Phys. Rev. B* **46**, 5100 (1992); Y. Ueda and D. K. Saldin, *ibid.* **46**, 13 697 (1992).
- <sup>11</sup>A. Santoni, A. Derossi, P. Finetti, R. G. Agostino, and B. Luo, *Phys. Rev. B* **46**, 15 660 (1992).
- <sup>12</sup>P. E. Batson and J. Bruley, *Phys. Rev. Lett.* **67**, 350 (1991).
- <sup>13</sup>O. Bisi, L. Braicovich, C. Carbone, I. Lindau, A. Iandelli, G. L. Olcese, and A. Palenzona, *Phys. Rev. B* **40**, 10 194 (1989).
- <sup>14</sup>C. Chemelli, M. Sancrotti, L. Braicovich, F. Ciccacci, O. Bisi, A. Iandelli, G. L. Olcese, and A. Palenzona, *Phys. Rev. B* **40**, 10 210 (1989).
- <sup>15</sup>D. D. Sarma, W. Speier, L. Kumar, C. Carbone, A. Spinsanti, O. Bisi, A. Iandelli, G. L. Olcese, and A. Palenzona, *Z. Phys.* **71**, 69 (1988).
- <sup>16</sup>Massimo Sancrotti, Ivano Abbati, Lucia Calliari, Fabio Marchetti, O. Bisi, A. Iandelli, G. L. Olcese, and A. Palenzona, *Phys. Rev. B* **37**, 4805 (1988); L. Calliari, F. Marchetti, M. Sancrotti, O. Bisi, A. Iandelli, G. L. Olcese, and A. Palenzona, *ibid.* **41**, 7569 (1990).
- <sup>17</sup>F. J. Himpsel, U. O. Karlsson, J. F. Morar, D. Rieger, and J. A. Yarmoff, *Phys. Rev. Lett.* **56**, 1497 (1986).
- <sup>18</sup>D. Rieger, F. J. Himpsel, U. O. Karlsson, F. R. McFeely, J. F. Morar, and J. A. Yarmoff, *Phys. Rev. B* **34**, 7295 (1986).
- <sup>19</sup>J. F. Morar and M. Wittmer, *Phys. Rev. B* **37**, 2618 (1988).
- <sup>20</sup>Massimo Sancrotti, Angela Rizzi, and Fabio Marchetti, *Phys. Rev. B* **37**, 3120 (1988).
- <sup>21</sup>C. Chemelli, S. Luridiana, M. Sancrotti, L. Braicovich, F. Ciccacci, A. Iandelli, G. L. Olcese, and A. Palenzona, *Phys. Rev. B* **42**, 1829 (1990).
- <sup>22</sup>M. Sancrotti, A. Iandelli, G. L. Olcese, and A. Palenzona, *Phys. Rev. B* **44**, 3328 (1991).
- <sup>23</sup>O. K. Andersen, *Phys. Rev. B* **12**, 3060 (1975).
- <sup>24</sup>P. Hohenberg and W. Kohn, *Phys. Rev.* **136**, B864 (1964); W. Kohn and L. Sham, *ibid.* **140**, A1133 (1965).
- <sup>25</sup>J.-P. Jan and H. L. Skriver, *J. Phys. F* **11**, 805 (1981).
- <sup>26</sup>P. J. W. Weijs *et al.*, *Phys. Rev. B* **41**, 11 899 (1990).
- <sup>27</sup>R. W. Wyckoff, *Crystal Structures* (Wiley, New York, 1963).
- <sup>28</sup>O. Jepsen and O. K. Andersen, *Solid State Commun.* **9**, 1763 (1971).
- <sup>29</sup>H. A. Bethe, *Ann. Phys. (Leipzig)* **5**, 325 (1930).
- <sup>30</sup>M. Inokuti, *Rev. Mod. Phys.* **43**, 297 (1971).
- <sup>31</sup>M. De Crescenzi, *J. Vac. Sci. Technol. A* **5**, 869 (1987); M. De Crescenzi, *CRC Crit. Rev. Solid State Mater. Sci.* **15**, 279 (1989); T. Tyliczszak and A. P. Hitchcock, *J. Vac. Sci. Technol. A* **8**, 2552 (1990).
- <sup>32</sup>P. E. Batson and J. Bruley, *Phys. Rev. Lett.* **67**, 350 (1991).
- <sup>33</sup>G. Paolucci, A. Santoni, G. Comelli, K. C. Prince, and R. G. Agostino, *Phys. Rev. B* **44**, 10 888 (1991).
- <sup>34</sup>O. Bisi, O. Jepsen, and O. K. Andersen, *Phys. Rev. B* **36**, 9439 (1987).
- <sup>35</sup>No significant chemical shift of the Ca 2*p* level has been observed with PES in Ca<sub>2</sub>Si. Carlo Carbone (private communication).
- <sup>36</sup>J. E. Muller *et al.*, *Phys. Rev. Lett.* **40**, 720 (1978); *Solid State Commun.* **42**, 365 (1982); J. E. Muller and J. W. Wilkins, *Phys. Rev. B* **29**, 4331 (1984).
- <sup>37</sup>C. J. Powell and N. E. Erickson, *Phys. Rev. Lett.* **51**, 61 (1983).
- <sup>38</sup>N. E. Erickson and C. J. Powell, *J. Vac. Sci. Technol. A* **1**, 1165 (1983).